Geochemical Perspectives Letters

Fluid-mediated uranium isotope fractionation in magmatic systems

J.-R. Sheng[1], D.-S. Jiang[1*], S. Erdmann[2], G.-X. Deng[1], H.-C. Duan[1], M. Jackson[3], G. Devos[4], F. Moynier[5], H.-H. Guo[6], F. Huang[1,7*]

Abstract

https://doi.org/10.7185/geochemlet.2525

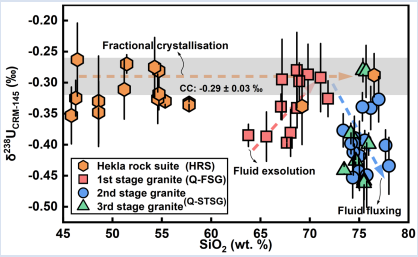

Uranium isotopes fractionation behaviour during magmatic differentiation and magmatic-hydrothermal processes remains unclear. In this study, we investigate two distinct magmatic systems: the Hekla rock suite (Iceland), which show basaltic to rhyolitic differentiation, and the Qitianling granites (South China), which show fluid modulated evolution. Our results show distinct U isotopic behaviours: although the $\delta^{238}U$ of the Hekla suite is variable (−0.35 ± 0.05 ‰ to −0.26 ± 0.06 ‰; 2 s.d.), it exhibits no correlation with differentiation indices, suggesting limited U isotope fractionation during magmatic differentiation. In contrast, the Qitianling granite show systematic $\delta^{238}U$ variations that we link to fluid related processes. Less evolved Qitianling granites (−0.34 ± 0.09 ‰) record ^{238}U enrichment in residual melts through fluid exsolution, whereas more evolved granites (−0.40 ± 0.10 ‰) exhibit lower $\delta^{238}U$ because of fluxing by ^{235}U-enriched fluids. These findings demonstrate that variations in $\delta^{238}U$ within magmatic systems are primarily governed by fluid related processes rather than by magmatic differentiation. Consequently, U isotopes have the potential to distinguish between these two processes, highlighting their value as tracers for magmatic-hydrothermal activity and fluid mediated transport of critical metals.

Received 20 February 2025 | Accepted 22 June 2025 | Published 4 August 2025

Introduction

Uranium (U), with an atomic number of 92, is the heaviest naturally occurring element on Earth. Its distinctive geochemical properties make it central to studies of magmatic and hydrothermal processes. Uranium is radioactive, with three primary naturally occurring isotopes: ^{238}U (99.2742 %), ^{235}U (0.7204 %), and ^{234}U (0.0054 %) (Meija *et al.*, 2016). The decay of ^{238}U and ^{235}U into ^{206}Pb and ^{207}Pb, respectively, underpins U-Pb geochronology, a cornerstone of Earth sciences. The difference in half-lives between ^{238}U ($t_{1/2}$ ≈ 4468 Myr) and ^{235}U ($t_{1/2}$ ≈ 703.7 Myr) has led to an increase in the $^{238}U/^{235}U$ value from ~3.3 to ~137.88 over Earth's 4.56 Gyr evolution (Andersen *et al.*, 2017). This ratio has traditionally been assumed to be constant, given the small mass difference between ^{238}U and ^{235}U, which supports Pb-Pb geochronology. However, small but measurable variations in $^{238}U/^{235}U$, expressed as $\delta^{238}U$ relative to the CRM-145 standard, have been recently observed (Weyer *et al.*, 2008; Voinot *et al.*, 2024). These variations are primarily attributed to the nuclear field shift associated with U isotope exchange during redox equilibration, representing stable U isotope fractionation (Bigeleisen, 1996; Weyer *et al.*, 2008; Tissot and Dauphas, 2015; Andersen *et al.*, 2017; Li and Tissot, 2023).

Uranium isotopes are emerging as a powerful geochemical tool for investigating high temperature geological processes (*e.g.*, partial melting and crystallisation fractionation), particularly in granitic magmatic systems (*e.g.*, Weyer *et al.*, 2008; Andersen *et al.*, 2017; Tissot and Dauphas, 2015). While there is no U isotope fractionation in basalts from Lake Kilauea due to the strong U incompatibility in mafic magmas (Gaschnig *et al.*, 2021), some studies have reported significant $\delta^{238}U$ variations in granitic systems. For example, I-, S-, and A-type granites from the Lachlan Fold Belt (Australia) exhibit heterogeneous $\delta^{238}U$ (−0.50 ‰ to −0.21 ‰) (Telus *et al.*, 2012), with more differentiated granitoids showing even greater fractionation (Tissot and Ibañez-Mejia, 2021). Additionally, U-rich accessory minerals such as zircon, apatite, and titanite show considerable $\delta^{238}U$ variability in solution based MC-ICP-MS analyses — up to 3.7 ‰, 0.38 ‰, and 3.0 ‰, respectively (Hiess *et al.*, 2012; Tissot and Dauphas, 2015; Livermore *et al.*, 2018; Tissot *et al.*, 2019). LA-MC-ICP-MS analyses reveal even broader ranges, reaching 10.0 ‰ for zircon and 16.0 ‰ for titanite

1. State Key Laboratory of Lithospheric and Environmental Coevolution, University of Science and Technology of China, Hefei 230026, China
2. Université d'Orléans–CNRS/INSU–ISTO–BRGM, UMR 7327, Orléans, France State
3. University of California Santa Barbara, Department of Earth Science, Santa Barbara, CA 93106, USA
4. Institute of Environmental Geology and Geoengineering (IGAG), Consiglio Nazionale delle Ricerche (CNR), Via Sandro Botticelli 23, Milan 20133, Italy
5. Université Paris Cité, Institut de Physique du Globe de Paris, CNRS, 1 Rue Jussieu, Paris 75005, France
6. State Key Laboratory of Geological Processes and Mineral Resources, China University of Geosciences, Wuhan 430074, China
7. Institute of Deep Space Sciences, Deep Space Exploration Laboratory, Hefei 230088, China
* Corresponding authors (emails: D.-S. Jiang, dshjiang@ustc.edu.cn; F. Huang, fhuang@ustc.edu.cn)

(Yamamoto *et al.*, 2021). These findings suggest that igneous differentiation, particularly through the removal of U-rich accessory minerals or the change in U coordination environments during mineral crystallisation (Tissot *et al.*, 2017), may fractionate U isotopes of residual granitic melts. Furthermore, studies of pegmatites and global granite-related U deposits have shown that U-rich magmatic-hydrothermal fluids (MHF) tend to exhibit low $\delta^{238}U$, reaching as low as −0.97 ‰ (Chernyshev *et al.*, 2014; Li and Tissot, 2023; Sheng *et al.*, 2025). These observations imply that magmatic-hydrothermal processes can further fractionate U isotopes of granitic magmas, imparting a distinct $\delta^{238}U$ signature. Collectively, these studies highlight the potential of $\delta^{238}U$ as a tracer for granitic evolution and magmatic-hydrothermal mineralisation. However, the systematic fractionation behaviour of U isotopes during granitic magmatic differentiation and hydrothermal processes is not well constrained.

To solve this issue, we report $\delta^{238}U$ for the Hekla rock suite (HRS) (Iceland) and Qitianling granites (South China). The HRS consists of basalts through rhyolites that have evolved through fractional crystallisation from a single mafic parental magma (Chekol *et al.*, 2011). They differ from those of Kilauea Iki in that they span a much broader compositional range, including evolved high silica rhyolites. Importantly, isotopic evidence from Li, Zn, Mo, Tl, K, Ba, and Rb indicates that these rocks show no signs of hydrothermal alteration (Wang *et al.*, 2023), making them ideal candidates for investigating U isotope fractionation solely during magmatic differentiation. The Qitianling intrusion consists of three stages of coeval Jurassic granites with the second and third stage granites (Q-STSG) representing fractionated melts extracted from the underlying crystal mush, compositionally similar to the first stage granites (Q-FSG) (Huang *et al.*, 2019; Deng *et al.*, 2022). Recent studies have suggested that the Q-STSG have been fluxed by MHF likely at 600–650 °C, which have exsolved from the Q-FSG under magmatic conditions at ~650–800 °C (Huang *et al.*, 2019; Deng *et al.*, 2022; Hu *et al.*, 2024). These characteristics make the Qitianling granites suitable for examining the fractionation behaviour of U isotopes during hydrothermal processes. The partitioning of U into MHF is enhanced by elevated concentrations of F and Cl (Peiffert *et al.*, 1996). Therefore, in addition to $\delta^{238}U$, we also report F and Cl concentrations for the Qitianling granites.

Geological Background and Samples

Hekla volcano is located at the margin of the propagating South Iceland Volcanic Zone. It has been active since 1104 A.D. and has had 18 historic eruptions. Hekla erupted a broad range of magma compositions with SiO_2 varying from 45.84 % to 76.52 %, with compositions ranging from basalt to basaltic andesite, andesite, dacite, and rhyolite (Ranta *et al.*, 2021). The lavas have similar Sr-Nd isotope compositions, suggesting that they are cogenetic (Chekol *et al.*, 2011). Simple fractional crystallisation in a closed system from basaltic to rhyolitic magmas is postulated as the main differentiation mechanism (Geist *et al.*, 2021) though other petrogenetic models were also proposed (Ranta *et al.*, 2021).

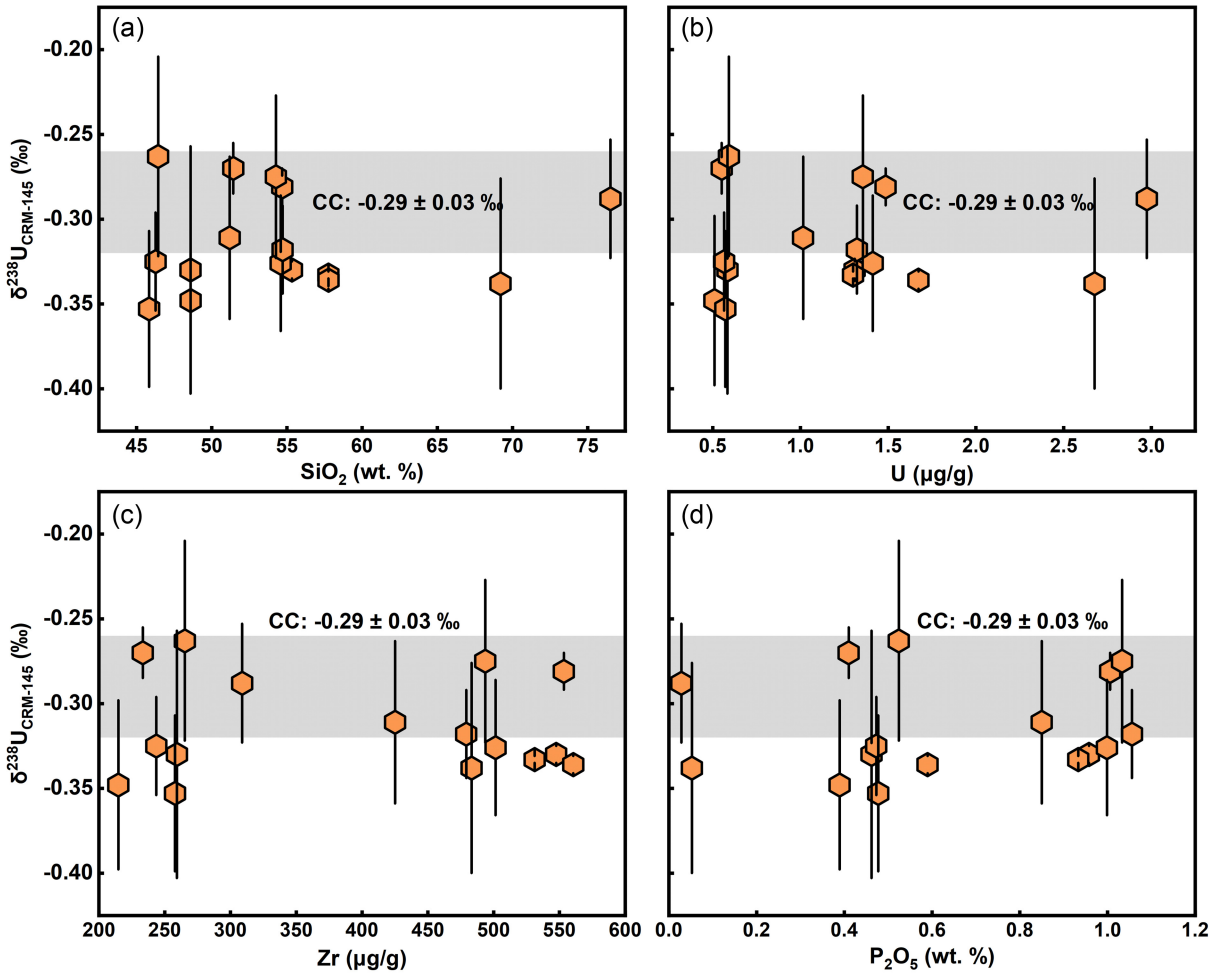

Figure 1 Co-variation of $\delta^{238}U$ *vs.* major and trace compositions of the Hekla rock suite. The $\delta^{238}U$ of the continental crust is from Tissot and Dauphas (2015).

The Qitianling batholith with a surface exposure of ~520 km^2 is located within the South China Block (Fig. S-1a). Field observations suggest that the batholith has three main magmatic stages defined by three distinct lithologies and contact relationships (Chen *et al.*, 2023). The Q-FSG are coarse grained porphyritic amphibole-biotite-rich granites (~45 %), while the Q-STSG are medium grained biotite ± amphibole granites (~40 %) and fine grained alkali-feldspar granites (~15 %), respectively. Field observations and zircon U-Pb dating indicate that these granite stages crystallised coevally at 150–160 Ma (Chen *et al.*, 2023). The whole rock $\varepsilon_{Nd}(t)$ (−5.5 to −8.9) of the granites are indistinguishable, implying the same crustal sources (Chen *et al.*, 2023). Phase equilibrium experiments and trace element modelling suggest that the Qitianling first, second, and third stage granites have compositions that fall along a continuous liquid line of descent (Huang *et al.*, 2019; Chen *et al.*, 2023).

Results

The δ^{238}U values for samples from Hekla and Qitianling are listed in Tables S-1 and S-2. The analytical methodology is provided in the Supplementary Information. The δ^{238}U of the HRS ranges from −0.35 ± 0.05 ‰ to −0.26 ± 0.06 ‰, closely comparable to those of Kilauea basalts (−0.38 ± 0.07 ‰ to −0.20 ± 0.06 ‰) (Gaschnig *et al.*, 2021). Although the δ^{238}U is variable, it exhibits no correlation with differentiation indices, such as SiO_2, U, Zr, or P_2O_5 concentrations (Fig. 1).

Fluorine and Cl concentrations of the Q-FSG range from 1240 to 2805 μg/g and 220 to 786 μg/g, respectively, which are well correlated with U/Th and K/Rb values (Fig. 2). Notably, the F (2233 to 7046 μg/g) and Cl (65.6 to 281 μg/g) concentrations of the Q-STSG are much higher or lower than those in the Q-FSG, respectively.

The δ^{238}U in the Q-FSG varies from −0.40 ± 0.00 ‰ to −0.28 ± 0.06 ‰, with an average of −0.34 ± 0.09 ‰. These values increase with increasing SiO_2 (and $Fe^{3+}/\Sigma Fe$) and decreasing MgO, ΣFe, F, Cl, U/Th, and Sn/Sm (Figs. 2, 3). Although the δ^{238}U range of the Q-STSG (−0.46 ± 0.03 ‰ to −0.28 ± 0.02 ‰ with an average of −0.40 ± 0.10 ‰) overlaps with that of the Q-FSG, a *t* test reveals a statistically significant difference between the groups ($p = 0.002$). Moreover, Q-STSG samples tend to exhibit lower $\delta^{138/134}$Ba, K/Rb, and Zr/Hf ratios, along with higher Na_2O contents, relative to Q-FSG (Fig. 4).

Discussion

Uranium isotope fractionation during igneous differentiation. Typically, U behaves incompatibly during fractional crystallisation with a partition coefficient ($D_U^{solid/melt}$) of 0.0011 (Workman and Hart, 2005) and is thus concentrated in residual melts. This incompatible behaviour is also evident in the

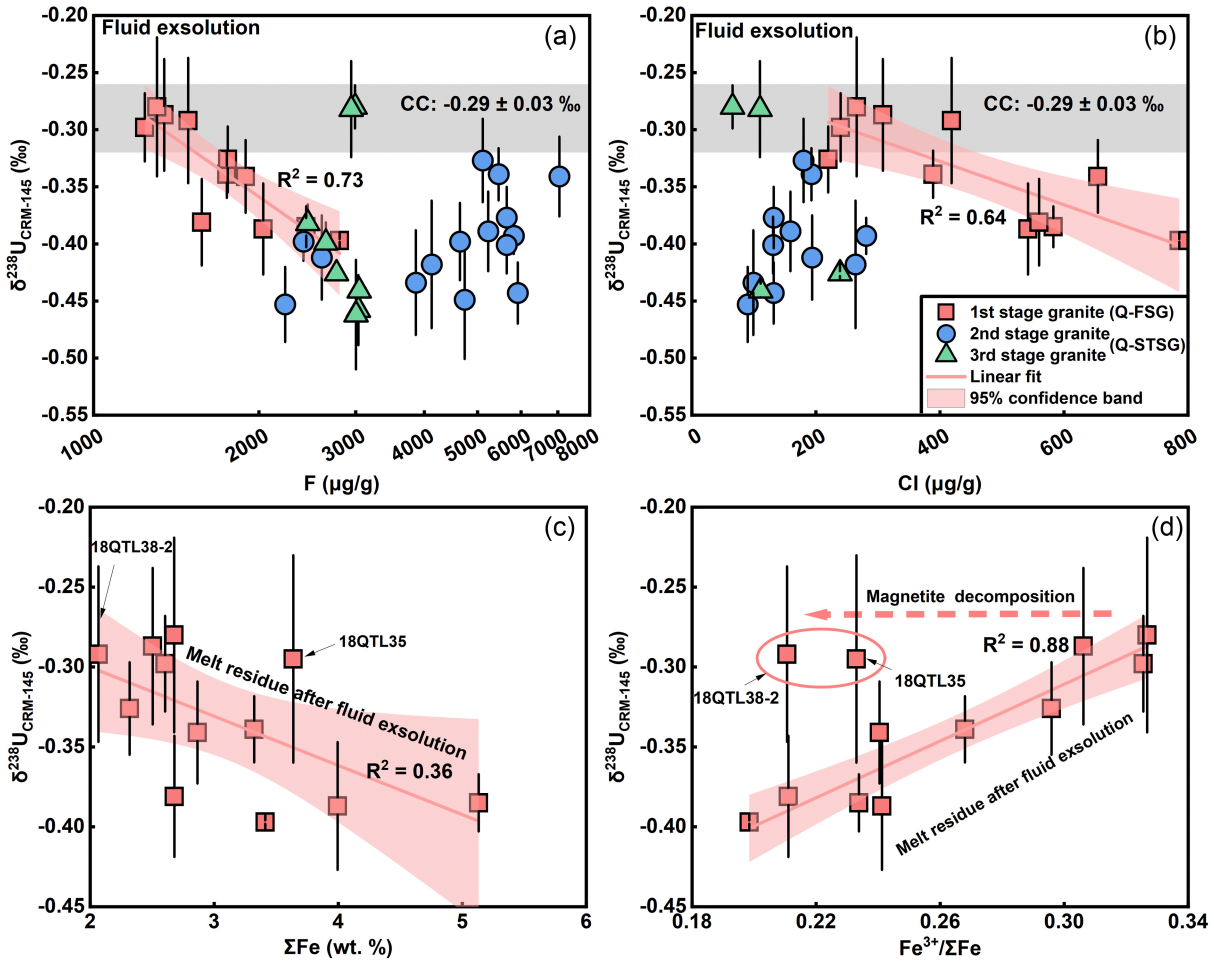

Figure 2 Positive or negative correlations between δ^{238}U with geochemical compositions for the Qitianling granites. Continued exsolution of Fe^{2+}-rich fluids oxidises Q-FSG melts and reduces FeO concentrations. Ultimately, this process can destabilise early crystallised magnetite evidenced in samples 18QTL35 and 18QTL38-2.

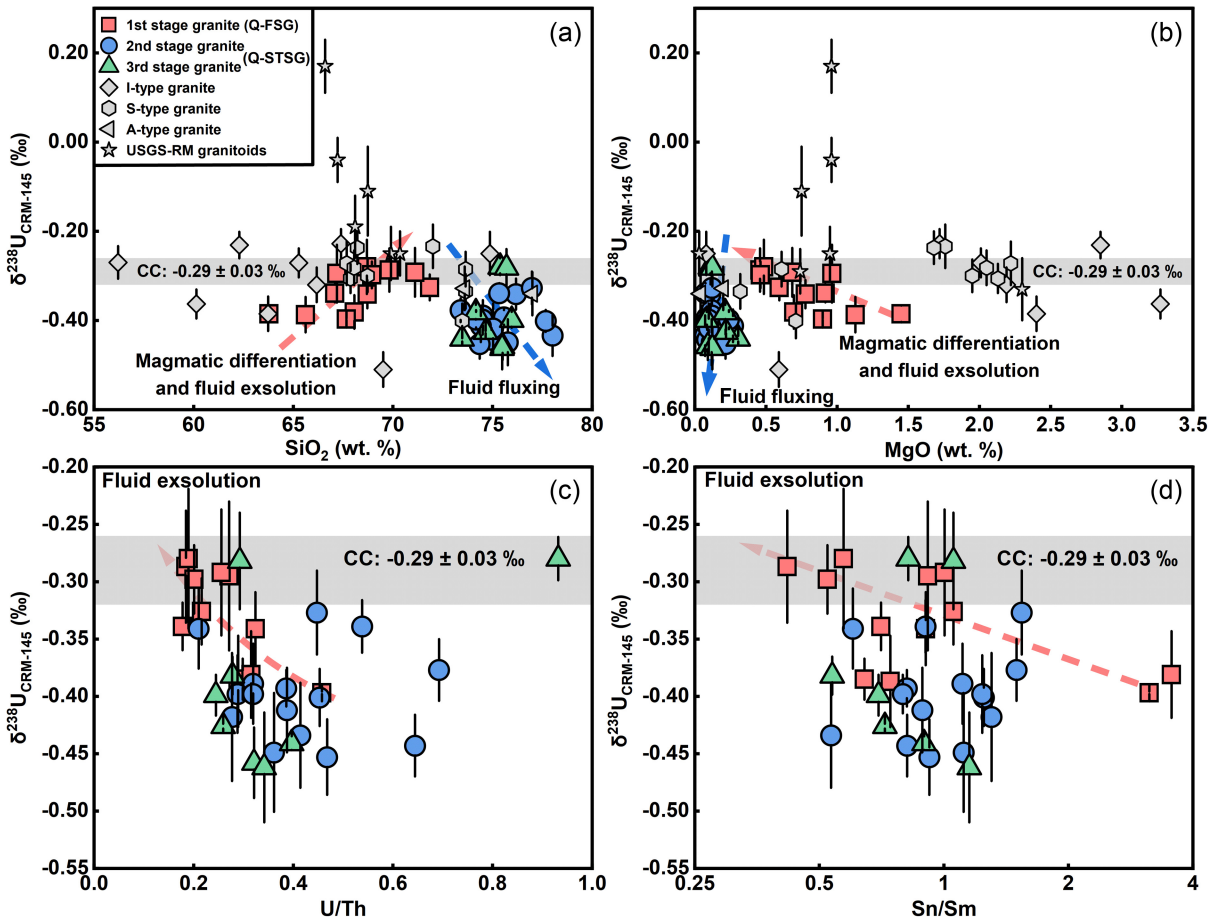

Figure 3 Plots of $\delta^{238}U$ *vs.* **(a)** SiO_2, **(b)** MgO, **(c)** U/Th and **(d)** Sn/Sm compositions for the Qitianling granites. Data for other granites are from Telus *et al.* (2012) and Li and Tissot (2023).

monotonic correlations between concentrations of U and major or trace elements of the HRS (Fig. S-2a–f). However, in the Hekla magmas, zircon and apatite have fractionated, as indicated by decreased Zr concentrations at ~65 wt. % SiO_2 and decreased P_2O_5 concentrations at ~54 wt. % SiO_2 (Fig. S-2g,h). Zircon and apatite are significant U-rich accessory minerals in felsic magmas. Their removal, particularly given their enrichment in ^{238}U relative to crustal rocks (Hiess *et al.*, 2012; Livermore *et al.*, 2018; Tissot *et al.*, 2019; Tissot and Ibañez-Mejia, 2021), may enrich the residual melts in ^{235}U. Nevertheless, although the $\delta^{238}U$ of the HRS is variable, it exhibits no correlation with differentiation indices, such as SiO_2, U, Zr, or P_2O_5 concentrations (Fig. 1). These trends suggest that U isotope fractionation during granitic differentiation is minimal, even when U-rich accessory phases are removed. The observed $\delta^{238}U$ variability in the Hekla basalts may reflect heterogeneity of the mantle source which could contain minor recycled crustal material (Halldórsson *et al.*, 2016) or reflect interactions between the Icelandic plume and the Mid-Atlantic Ridge (Schilling, 1973). As U isotopes are insignificantly fractionated during fractional crystallisation, we further hypothesise that they are not fractionated during the partial melting of crust and mantle either, which involves mineral melting followed by melt separation. This interpretation is supported by the identical $\delta^{238}U$ estimated for bulk crust and mantle compositions (Tissot and Dauphas, 2015).

Uranium isotope fractionation during fluid exsolution. Magmatic-hydrothermal fluids play a critical role in migrating U from granitic magmas (Zajacz *et al.*, 2008). Phase equilibrium experiments suggest that the Q-FSG has a solidus of 650 °C and a liquidus above 900 °C (Huang *et al.*, 2019). They also imply that parental magmas of the Q-FSG were initially H_2O-rich (≥4 wt. %) and reached water saturation (~6.5–8.0 wt. %) at ≤300 MPa and 800 °C. However, the loss on ignition (LOI) of the Q-FSG is low (~0.42 to 0.86 wt. %). Moreover, miarolitic cavities, typically indicating the entrapment of fluid-rich melts or hydrosaline fluids, are absent in the Q-FSG, and evidence of hydrothermal alteration is minimal (Huang *et al.*, 2019). These observations suggest that the exsolution and subsequent loss of MHF occurred during the magmatic evolution of the Q-FSG magmas, likely within a temperature window of ~650–800 °C

This hypothesis is further supported by other bulk rock geochemical trends.

1. **Uranium concentrations**. In granitic melts, U concentrations typically increase with magmatic differentiation, even when U-rich accessory phases are fractionated (Fig. S-2a–d). However, in the Q-FSG, U concentrations remained constant during magmatic evolution (Fig. S-3). Uranium can be a fluid mobile element, and its concentration in magmas decreases during the exsolution of F (Cl)-rich fluids (Peiffert *et al.*, 1996). Therefore, the consistent U concentrations can result from a compensatory effect involving fractional crystallisation and fluid exsolution.
2. **Fluid mobile *vs.* fluid incompatible element ratios**. K and Rb, U, and Th, as well as Sn and Sm, exhibit similar compatibility during magmatic differentiation. Thus,

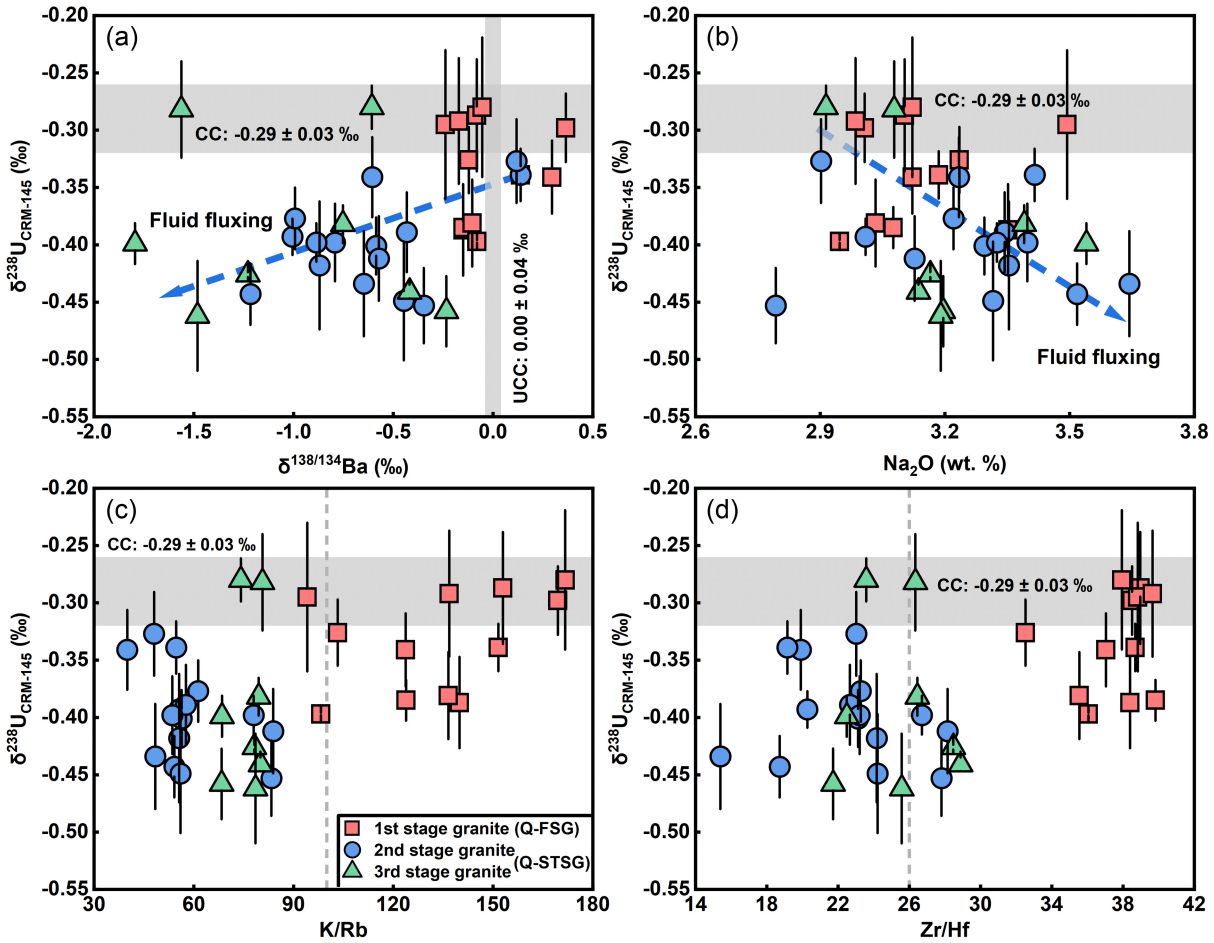

Figure 4 The $\delta^{238}U$ *vs.* **(a)** $\delta^{138}Ba$, **(b)** Na_2O, **(c)** K/Rb and **(d)** Zr/Hf compositions of the Qitianling granites. The vertical grey field indicates the average $\delta^{138/134}Ba$ of the UCC (Deng *et al.*, 2022 and references therein).

fractional crystallisation cannot substantially change K/Rb, Rb/Sr, U/Th, and Sn/Sm ratios in magmas. However, during the magmatic evolution of the Q-FSG, the K/Rb ratio increases, while the Rb/Sr, U/Th, and Sn/Sm ratios decrease (Fig. S-4a–d). This pattern can be attributed to variable loss of these elements during fluid exsolution due to their different fluid mobilities. For example, Rb, U, and Sn are more fluid mobile than K, Th, and Sm (Zajacz *et al.*, 2008), respectively. Moreover, Rb is more incompatible and more fluid mobile than Sr (Zajacz *et al.*, 2008). Fluid exsolution preferentially partitions Rb, U, and Sn into the MHF, leaving behind a melt enriched in K, Th, and Sm.

3. **F-Cl concentrations**. The Q-FSG have variable F and Cl concentrations which show positive correlations with the U/Th ratio and negative correlations with the K/Rb ratio (Fig. S-5). These trends deviate from the typical patterns expected during fractional crystallisation. Instead, they are consistent with the exsolution of F- and Cl-rich MHF in the Qitianling magmatic system, which is known to be enriched in F, Cl, U, and Rb (Chen *et al.*, 2023).

4. **$Fe^{3+}/\Sigma Fe$ ratio**. The $Fe^{3+}/\Sigma Fe$ ratio of the Q-FSG increases with magmatic evolution but shows no correlation with SiO_2 or $Fe_2O_3^T$ concentrations (Fig. S-6). These observations suggest that the elevated $Fe^{3+}/\Sigma Fe$ ratio does not result from igneous differentiation. Experimental studies indicate that the exsolution of Cl-bearing fluids removes Fe^{2+} over Fe^{3+} from melts, thereby increasing the $Fe^{3+}/\Sigma Fe$ ratio in residual melts (Bell and Simon, 2011). In the Q-FSG magmas, this interpretation is supported by correlations between $Fe^{3+}/\Sigma Fe$ and K/Rb, Rb/Sr, U/Th, Sn/Sm, F, or Cl compositions (Fig. S-4a–f).

The Q-FSG exhibit a variable $\delta^{238}U$, which is lower than the averaged $\delta^{238}U$ of the continental crust (CC) (Fig. 2). Since U isotopes are not fractionated during continental weathering (Tissot and Dauphas, 2015), this isotopic variation must be attributed to magmatic and/or magmatic-hydrothermal processes. Fractional crystallisation of U-rich minerals, such as zircon and apatite (Fig. S-7a,b), plays a key role in driving compositional variability in the Q-FSG (Deng *et al.*, 2022). However, as seen in the HRS (Fig. 1), U isotopes are also not fractionated during igneous differentiation, even when U-rich phases are fractionated. This suggests that the $\delta^{238}U$ variation in the Q-FSG is driven by processes beyond fractional crystallisation. As discussed earlier, the Q-FSG magmas experienced the exsolution and loss of U-rich MHF with the magmatic evolution. More importantly, the $\delta^{238}U$ of the Q-FSG shows correlations with SiO_2 and MgO, U/Th, Sn/Sm, F, Cl, ΣFe, and $Fe^{3+}/\Sigma Fe$ compositions (Figs. 2, 3). These correlations strongly indicate that the exsolution of MHF, which is inferred to be enriched in ^{235}U, was a key process driving the $\delta^{238}U$ fractionation in the Q-FSG. To quantify the fluid exsolution-induced U isotope fractionation, we performed a simulation using Rayleigh distillation models which successfully reproduces the observed $\delta^{238}U$ variation in the Q-FSG (Fig. S-8a).

Uranium isotope fractionation during fluid fluxing. The Q-STSG experienced greater magmatic differentiation and more extensive fluid exsolution compared to the Q-FSG (Huang *et al.*, 2019). Theoretically, this enhanced fluid exsolution should result in higher $\delta^{238}U$ in the residual melts. However, the $\delta^{238}U$ of the Q-STSG (−0.40±0.10 ‰) is lower than that of the Q-FSG (−0.34 ± 0.09 ‰), showing no consistent fractionation trend (Figs. 2, 3). This unexpected pattern indicates that fluid exsolution alone cannot account for the low $\delta^{238}U$ observed in the Q-STSG.

The Q-STSG exhibit extensive hydrothermal alterations and partial replacement of magmatic minerals such as biotite and titanite by chlorite and Fe-Ti oxides, respectively (Deng *et al.*, 2022; Hu *et al.*, 2024). These were driven by the fluxing of low $\delta^{138}Ba$ and high $\delta^{87}Rb$ MHF (Deng *et al.*, 2022; Hu *et al.*, 2024), which also contributed to the formation of the giant Sn deposit (SnO_2 > 700,000 tons) (Chen *et al.*, 2023). As shown in Figure 4a,b, the Q-STSG samples with low $\delta^{238}U$ also tend to have low $\delta^{138/134}Ba$ and elevated Na_2O concentrations, typical of ore-forming fluids in the Qitianling intrusion (Chen *et al.*, 2023). Additionally, these low $\delta^{238}U$ samples display low K/Rb and Zr/Hf (Fig. 4c,d), suggesting fluid-melt interaction which modified the melt composition in a way consistent with fluid-derived elemental ratios (*i.e.* low K/Rb and Zr/Hf) (Deng *et al.*, 2022). Based on these geochemical signatures, it is suggested that the fluxing of MHF fractionated the $\delta^{238}U$ of the resident magmas, resulting in the lower $\delta^{238}U$ signature of the Q-STSG. This interpretation is consistent with the enrichment of ^{235}U in MHF exsolved from the Q-FSG magmas. Moreover, this conclusion also aligns with the observation that granite-related hydrothermal U deposits typically exhibit lower $\delta^{238}U$ than the average CC (Chernyshev *et al.*, 2014), although some deposits show $\delta^{238}U$ indistinguishable from that of the CC (Voinot *et al.*, 2024). To quantify the fluid fluxing-induced U isotope fractionation, we performed open system modelling (Table S-4). The results show that the $\delta^{238}U$ of the Q-STSG can be reproduced using apparent fractionation factors ($\alpha_{fluid\text{-}melt}$) ranging from 0.9982 to 0.9996 (Fig. S-8b) which may depend on temperature and compositions of the melt and fluid.

Conclusions

This study investigated U isotope fractionation behaviour during magmatic differentiation and hydrothermal processes by analysing $\delta^{238}U$ in the Hekla rock suite and the Qitianling granites. Our results indicate that $\delta^{238}U$ variations in magmatic systems are primarily influenced by fluid related processes rather than magmatic differentiation. The atypical U isotope characteristics observed in granitoids may serve as a novel tracer for fluid related processes, offering valuable insights into the migration and enrichment of fluid mobile elements associated with magmatic-hydrothermal fluids.

Data availability

Data will be made available on request.

Acknowledgments

We sincerely acknowledge Prof. Sæmundur Ari Halldórsson for his invaluable academic discussions and intellectual contributions. Our profound gratitude also extends to François L.H. Tissot, the anonymous reviewer, and Editor Ambre Luguet, whose incisive critiques and professional guidance have substantially elevated the scholarly rigour and presentation of this work. This work was financially supported by the National Natural Science Foundation of China (Grant No. 42473010).

Editor: Ambre Luguet

Additional Information

Supplementary Information accompanies this letter at https://www.geochemicalperspectivesletters.org/article2525.

Cite this letter as: Sheng, J.-R., Jiang, D.-S., Erdmann, S., Deng, G.-X., Duan, H.-C., Jackson, M., Devos, G., Moynier, F., Guo, H.-H., Huang, F. (2025) Fluid-mediated uranium isotope fractionation in magmatic systems. *Geochem. Persp. Let.* 36, 1–7. https://doi.org/10.7185/geochemlet.2525

References

Andersen, M.B., Stirling, C.H., Weyer, S. (2017) Uranium Isotope Fractionation. *Reviews in Mineralogy and Geochemistry* 82, 799–850. https://doi.org/10.2138/rmg.2017.82.19

Bell, A.S., Simon, A. (2011) Experimental evidence for the alteration of the $Fe^{3+}/\Sigma Fe$ of silicate melt caused by the degassing of chlorine-bearing aqueous volatiles. *Geology* 39, 499–502. https://doi.org/10.1130/G31828.1

Bigeleisen, J. (1996) Nuclear Size and Shape Effects in Chemical Reactions. Isotope Chemistry of the Heavy Elements. *Journal of the American Chemical Society* 118, 3676–3680. https://doi.org/10.1021/ja954076k

Chekol, T.A., Kobayashi, K., Yokoyama, T., Sakaguchi, C., Nakamura, E. (2011) Timescales of magma differentiation from basalt to andesite beneath Hekla Volcano, Iceland: Constraints from U-series disequilibria in lavas from the last quarter-millennium flows. *Geochimica et Cosmochimica Acta* 75, 256–283. https://doi.org/10.1016/j.gca.2010.10.001

Chen, S.-C., Yu, J.-J., Bi, M.-F., Lehmann, B. (2023) Fluid-rock interaction and fluid mixing in the large Furong tin deposit, South China: New insights from tourmaline and apatite chemistry and in situ B-Nd-Sr isotope composition. *American Mineralogist* 108, 338–353. https://doi.org/10.2138/am-2022-8310

Chernyshev, I., Golubev, V., Chugaev, A., Baranova, A. (2014) $^{238}U/^{235}U$ isotope ratio variations in minerals from hydrothermal uranium deposits. *Geochemistry International* 52, 1013–1029. https://doi.org/10.1134/S0016702914120027

Deng, G., Jiang, D., Zhang, R., Huang, J., Zhang, X., Huang, F. (2022) Barium isotopes reveal the role of deep magmatic fluids in magmatic-hydrothermal evolution and tin enrichment in granites. *Earth and Planetary Science Letters* 594, 117724. https://doi.org/10.1016/j.epsl.2022.117724

Gaschnig, R.M., Rader, S.T., Reinhard, C.T., Owens, J.D., Planavsky, N., Wang, X., Asael, D., Greaney, A., Helz, R. (2021) Behavior of the Mo, Tl, and U isotope systems during differentiation in the Kilauea Iki lava lake. *Chemical Geology* 574, 120239. https://doi.org/10.1016/j.chemgeo.2021.120239

Geist, D., Harpp, K., Oswald, P., Wallace, P., Bindeman, I., Christensen, B. (2021) Hekla Revisited: Fractionation of a Magma Body at Historical Timescales. *Journal of Petrology* 62, egab001. https://doi.org/10.1093/petrology/egab001

Halldórsson, S.A., Hilton, D.R., Barry, P.H., Füri, E., Grönvold, K. (2016) Recycling of crustal material by the Iceland mantle plume: New evidence from nitrogen elemental and isotope systematics of subglacial basalts. *Geochimica et Cosmochimica Acta* 176, 206–226. https://doi.org/10.1016/j.gca.2015.12.021

Hiess, J., Condon, D.J., McLean, N., Noble, S.R. (2012) $^{238}U/^{235}U$ Systematics in Terrestrial Uranium-Bearing Minerals. *Science* 335, 1610–1614. https://doi.org/10.1126/science.1215507

Hu, X., Jiang, D., Deng, G., Huang, F. (2024) Rubidium isotope compositions of biotite in granites record magmatic-hydrothermal process and rare metal enrichments. *Geochimica et Cosmochimica Acta* 382, 26–39. https://doi.org/10.1016/j.gca.2024.08.006

Huang, F., Scaillet, B., Wang, R., Erdmann, S., Chen, Y., Faure, M., Liu, H., Xie, L., Wang, B., Zhu, J. (2019) Experimental Constraints on Intensive Crystallization Parameters and Fractionation in A-Type Granites: A Case Study on the Qitianling Pluton, South China. *Journal of Geophysical Research: Solid Earth* 124, 10132–10152. https://doi.org/10.1029/2019JB017490

Li, H., Tissot, F.L.H. (2023) UID: The uranium isotope database. *Chemical Geology* 618, 121221. https://doi.org/10.1016/j.chemgeo.2022.121221

Livermore, B.D., Connelly, J.N., Moynier, F., Bizzarro, M. (2018) Evaluating the robustness of a consensus $^{238}U/^{235}U$ value for U-Pb geochronology. *Geochimica et Cosmochimica Acta* 237, 171–183. https://doi.org/10.1016/j.gca.2018.06.014

Meija, J., Coplen, T.B., Berglund, M., Brand, W.A., De Bièvre, P., Gröning, M., Holden, N.E., Irrgeher, J., Loss, R.D., Walczyk, T., Prohaska, T. (2016) Isotopic compositions of the elements 2013 (IUPAC Technical Report). *Pure and Applied Chemistry* 88, 293–306. https://doi.org/10.1515/pac-2015-0503

Peiffert, C., Nguyen-Trung, C., Cuney, M. (1996) Uranium in granitic magmas: Part 2. Experimental determination of uranium solubility and fluid-melt partition coefficients in the uranium oxide-haplogranite-H_2O-NaX (X = Cl, F) system at 770°C, 2 kbar. *Geochimica et Cosmochimica Acta* 60, 1515–1529. https://doi.org/10.1016/0016-7037(96)00039-7

Ranta, E., Halldórsson, S.A., Barnes, J.D., Jónasson, K., Stefánsson, A. (2021) Chlorine isotope ratios record magmatic brine assimilation during rhyolite genesis. *Geochemical Perspectives Letters* 16, 35–39. https://doi.org/10.7185/geochemlet.2101

Schilling, J.-G. (1973) Iceland Mantle Plume: Geochemical Study of Reykjanes Ridge. *Nature* 242, 565–571. https://doi.org/10.1038/242565a0

Sheng, J., Quan, Y., Jiang, D., Deng, G., Li, G., Xu, Z., Huang, F. (2025) Uranium isotope fractionation during magmatic-hydrothermal interactions in pegmatites. *Chemical Geology* 677, 122632. https://doi.org/10.1016/j.chemgeo.2025.122632

Telus, M., Dauphas, N., Moynier, F., Tissot, F.L.H., Teng, F.-Z., Nabelek, P.I., Craddock, P.R., Groat, L.A. (2012) Iron, zinc, magnesium and uranium isotopic fractionation during continental crust differentiation: The tale from migmatites, granitoids, and pegmatites. *Geochimica et Cosmochimica Acta* 97, 247–265. https://doi.org/10.1016/j.gca.2012.08.024

Tissot, F.L.H., Dauphas, N. (2015) Uranium isotopic compositions of the crust and ocean: Age corrections, U budget and global extent of modern anoxia. *Geochimica et Cosmochimica Acta* 167, 113–143. https://doi.org/10.1016/j.gca.2015.06.034

Tissot, F.L.H., Ibañez-Mejia, M. (2021) Unlocking the Single-Crystal Record of Heavy Stable Isotopes. *Elements* 17, 389–394. https://doi.org/10.2138/gselements.17.6.389

Tissot, F.L.H., Dauphas, N., Grove, T.L. (2017) Distinct $^{238}U/^{235}U$ ratios and REE patterns in plutonic and volcanic angrites: Geochronologic implications and evidence for U isotope fractionation during magmatic processes. *Geochimica et Cosmochimica Acta* 213, 593–617. https://doi.org/10.1016/j.gca.2017.06.045

Tissot, F.L.H., Ibanez-Mejia, M., Boehnke, P., Dauphas, N., McGee, D., Grove, T.L., Harrison, T.M. (2019) $^{238}U/^{235}U$ measurement in single-zircon crystals: implications for the Hadean environment, magmatic differentiation and geochronology. *Journal of Analytical Atomic Spectrometry* 34, 2035–2052. https://doi.org/10.1039/C9JA00205G

Voinot, A., Kyser, T.K., Chipley, D., Valentino, M., Uvarova, Y., Layton-Matthews, D., Leybourne, M.I. (2024) Tl, Mo and U isotopes in U-ore deposits record Earth's fundamental redox processes. *Chemical Geology* 661, 122154. https://doi.org/10.1016/j.chemgeo.2024.122154

Wang, B., Moynier, F., Jackson, M.G., Huang, F., Hu, X., Halldórsson, S.A., Dai, W., Devos, G. (2023) Rubidium isotopic fractionation during magmatic processes and the composition of the bulk silicate Earth. *Geochimica et Cosmochimica Acta* 354, 38–50. https://doi.org/10.1016/j.gca.2023.05.021

Weyer, S., Anbar, A.D., Gerdes, A., Gordon, G.W., Algeo, T.J., Boyle, E.A. (2008) Natural fractionation of $^{238}U/^{235}U$. *Geochimica et Cosmochimica Acta* 72, 345–359. https://doi.org/10.1016/j.gca.2007.11.012

Workman, R.K., Hart, S.R. (2005) Major and trace element composition of the depleted MORB mantle (DMM). *Earth and Planetary Science Letters* 231, 53–72. https://doi.org/10.1016/j.epsl.2004.12.005

Yamamoto, K., Asanuma, H., Takahashi, H., Hirata, T. (2021) *In situ* isotopic analysis of uranium using a new data acquisition protocol for 10^{13} ohm Faraday amplifiers. *Journal of Analytical Atomic Spectrometry* 36, 668–675. https://doi.org/10.1039/D0JA00498G

Zajacz, Z., Halter, W.E., Pettke, T., Guillong, M. (2008) Determination of fluid/melt partition coefficients by LA-ICPMS analysis of co-existing fluid and silicate melt inclusions: Controls on element partitioning. *Geochimica et Cosmochimica Acta* 72, 2169–2197. https://doi.org/10.1016/j.gca.2008.01.034